

Techno-economic and environmental analysis of a grid-connected rooftop solar photovoltaic system in three climate zones

Tao Hai^{1,2,3}, Hussein A. Jaffar⁴, Hameed H. Taher⁵, Ameer H. Al-Rubaye⁶, Esraa Ahmed Said⁷, Abbas Hameed Abdul Hussein⁸, Wesam Abed AL Hassan Alhaidry⁹, Ameer Hassan Idan¹⁰, Abozar Salehi^{11,*} 

¹School of Information and Artificial Intelligence, Nanchang Institute of Science & Technology, Nanchang 330108, China

²School of Computer and Information, Qiannan Normal University for Nationalities, Duyun, Guizhou 558000, China

³Artificial Intelligence Research Center (AIRC), Ajman University, P.O. Box 346, Ajman, UAE

⁴Air Conditioning Engineering Department, Faculty of Engineering, Warith Al-Anbiyaa University, Iraq

⁵Al-Amarah University College, Maysan, Iraq

⁶Department of Petroleum Engineering, Al-Kitab University, Altun Kupri, Iraq

⁷College of Dentistry, Alnoor University, Mosul, Iraq

⁸Ahl Al Bayt University, Kerbala, Iraq

⁹College of Technical Engineering, National University of Science and Technology, Dhi Qar 64001, Iraq

¹⁰Al-Zahrawi University College, Karbala, Iraq

¹¹School of Engineering, Department of Environment, University of Tehran, Tehran, Iran

*Corresponding author. School of Engineering, Department of Environment, University of Tehran, Tehran, Iran. E-mail: salehi1054@ut.ac.ir

Abstract

This study aims to fill a gap in research on technical-economic and environmental assessments of grid-connected photovoltaic (PV) panels for residential electricity supply. To combat this, a study examines the feasibility of grid-connected rooftop solar PV systems in three cities. Using PVsyst software, technical, economic, and environmental factors were analyzed, including energy injected into the grid, net present value (NPV), internal rate of return (IRR), levelized cost of energy (LCOE), and life cycle emissions. It is concluded from this study that PV power plants are technically, economically, and environmentally feasible for all three climate zones, but cold zone with the highest annual production of 10.66 MWh, the highest NPV (\$5449.47), the highest IRR (14.28%), and the lowest LCOE (\$0.063/kWh) is the most appropriate place to set up a PV power plant (Scenario 1: No tracking system). Furthermore, using horizontal (Scenario 2), vertical (Scenario 3), and two-axis tracking (Scenario 4) systems instead of the no-tracking system (Scenario 1) increases the amount of electricity injected into the grid by 7.56%, 24.67%, and 36.35%, respectively. According to life cycle emission, the annual production of 10.66 MWh by the 5 kW power plant installed in cold zone will prevent 102.02 tons of carbon dioxide emissions into the atmosphere (Scenario 1: No tracking system). To remove financial obstacles and increase the viability of renewable energy, the government must provide financial incentives, lower the cost of equipment, and enact strong renewable energy legislation.

Keywords: grid-connected rooftop photovoltaic; solar tracking; techno-economic analysis; Levelized cost of energy; life cycle emissions

Introduction

Increased population and industrialization have heightened the urgency for environmental security, energy conservation, and sustainable energy [1, 2]. Scientists globally are pursuing renewable energy as traditional fossil resources decline [3]. Among these, solar energy, deriving from the sun the most plentiful renewable resource, stands out as a prime alternative [4, 5]. In the past decade, the average cost of photovoltaic (PV) technologies has decreased significantly, by approximately 1.5 \$/Wp (an 80% reduction), with annual PV installations projected to hit 1 TW between 2025 and 2028 [6]. Solar energy is being increasingly utilized in various sectors. For example, in agriculture, solar-powered water pumps are predominantly used for irrigation, rendering the system independent of the power grid [7, 8]. In the construction industry, solar energy is employed for diverse applications such as

air conditioning [9], water heating [10], lighting [11], and powering cooling devices [12].

Another crucial application of solar power is in the field of water desalination, where electricity generated from solar plants is used to produce low-salinity water from saltwater [13, 14]. There are two desalination methods: heating saltwater and membranes. Solar power benefits telecom via satellites [15]. Solar energy is also commonly used as a backup power source in fixed telecommunications networks [16]. Regarding sustainable energy solutions, the generation and utilization of hydrogen through water electrolysis present promising methods for achieving decarbonization by 2050 [17]. Notably, solar energy has been identified as the most cost-effective and environmentally friendly option for powering electrolysis processes [18]. In the context of global energy dynamics, Iran ranks as the 19th largest power

Received 26 March 2024; revised 25 May 2024

© The Author(s) 2024. Published by Oxford University Press.

This is an Open Access article distributed under the terms of the Creative Commons Attribution Non-Commercial License (<https://creativecommons.org/licenses/by-nc/4.0/>), which permits non-commercial re-use, distribution, and reproduction in any medium, provided the original work is properly cited. For commercial re-use, please contact journals.permissions@oup.com

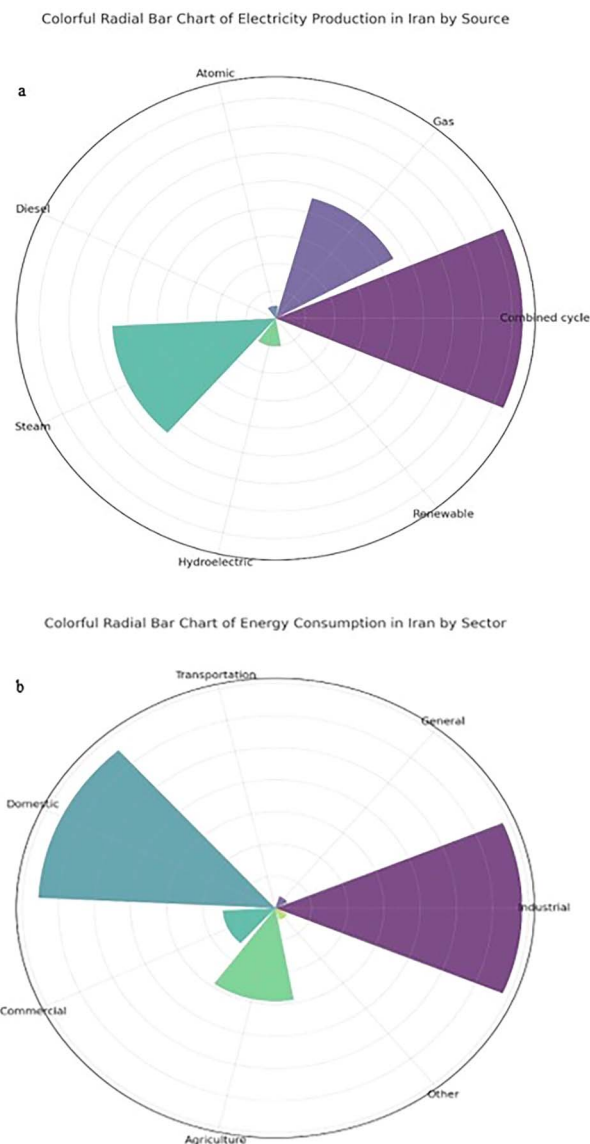


Figure 1. (a) Electricity production in Iran by source. (b) Energy consumption in Iran by sector [20].

producer and the 20th largest consumer of electricity [19]. According to the 2017 annual report of Iran's Ministry of Energy, a staggering 92.3% (285.4 TWh) of the country's total electricity generation is derived from fossil fuels, with a mere 0.3% sourced from alternative energies, as depicted in Fig. 1a [21].

Iran relies on the industry for economic growth and electricity consumption [20]. Iran's geographic location in South Asia, along with data from SATBA, shows its significant solar energy potential. With 300 sunny days per year and an average solar irradiation of 4.5–5.5 kWh/m²/day, Iran has ideal conditions for harnessing solar energy [22]. For instance, a study by Najafi *et al.* [22] indicates that with just 10% system efficiency, solar radiation could potentially produce approximately 9 million MWh of energy per day on merely 1% of Iran's total land area. Despite these promising figures, Iran's current solar power implementation is approximately 365 MW, contributing to less than 0.5% of its total energy consumption.

Bakhshi-Jafarabadi *et al.* [23] note that the levelized cost of energy (LCOE) of PV panels in Iran is currently considerably higher than the average electricity prices in residential, commercial, and industrial sectors. Government incentives promote solar plants and reduce emissions; PV panels improve efficiency [24]. Solar trackers with feedback control increase energy yield by 25%–40% [25]. Tracking devices are effective in boosting electricity generation in areas with high solar radiation like the Middle East [26]. Fixed panels are more affordable than tracking [27]. Therefore, these devices are more suitable for larger power plants and require extensive feasibility studies at local levels [28]. Koussa *et al.* [29] compared different trackers' performance in varied weather conditions, finding two-axis trackers excelled on clear days, while all trackers performed similarly on cloudy days. Singh *et al.* [30] explored the role of tracker devices in PV systems, discovering that single-axis sun trackers could enhance power output by 12% to 25%, and two-axis systems by 30% to 45%. Honrubia-Escribano *et al.* [31] highlighted that the economic benefits of solar trackers heavily rely on federal tariff policies, underscoring the importance of research on these systems in various global regions. Lastly, Bahrami and Okoye [32] assessed energy generation from various tracker devices in the northern hemisphere, finding that higher cost PV systems performed better with vertical-axis and full-axis trackers. Additionally, as latitude increased, north–south and vertical-axis horizontal axis trackers became more cost-effective. A study by Mohammadi *et al.* [33] on a PV plant in Iran's southern coast found the vertical-axis tracker to be the most efficient, with a COE of \$103–117.3/MWh. This 5 MW system could save 5259 tons of CO₂ yearly compared to gas power plants. Antonanzas *et al.* [34] found that single-axis trackers outperformed fixed systems in terms of environmental impact, specifically in carbon dioxide reduction.

Despite these studies, there is a noted gap in research on the technical-economic analysis and environmental assessments of grid-connected PV systems for residential areas in Iran, particularly under the climatic conditions of Fars province. This study aims to fill this gap, being the first comprehensive technical, economic, and environmental comparison of PV panels (grid-connected) for residential electricity supply in Fars province.

The primary objective of this research is to conduct a thorough evaluation of the performance of a 5 kW grid-connected rooftop solar PV system in residential districts of Fars province, considering its three climate zones. The study focuses on the efficiency of the system from technological, financial, and environmental perspectives. It involves a comparative analysis of different solar trackers in terms of technology, geography, and meteorology across the three climate zones to meet household power demands. Three regions in Fars province were selected as pilot areas to assess the impact of solar radiation and climatic conditions on the efficiency of solar trackers.

Moreover, this study includes an economic evaluation of four scenarios (with and without tracking systems) based on the Power Purchase Agreement (PPA) of Iran's Ministry of Energy, valid for 20 years from the start of the renewable power plant operation. Finally, it investigates the environmental implications, such as CO₂ emissions and savings in natural gas and water, of a 5 kW grid-connected rooftop solar PV system compared to conventional thermal power generation systems.

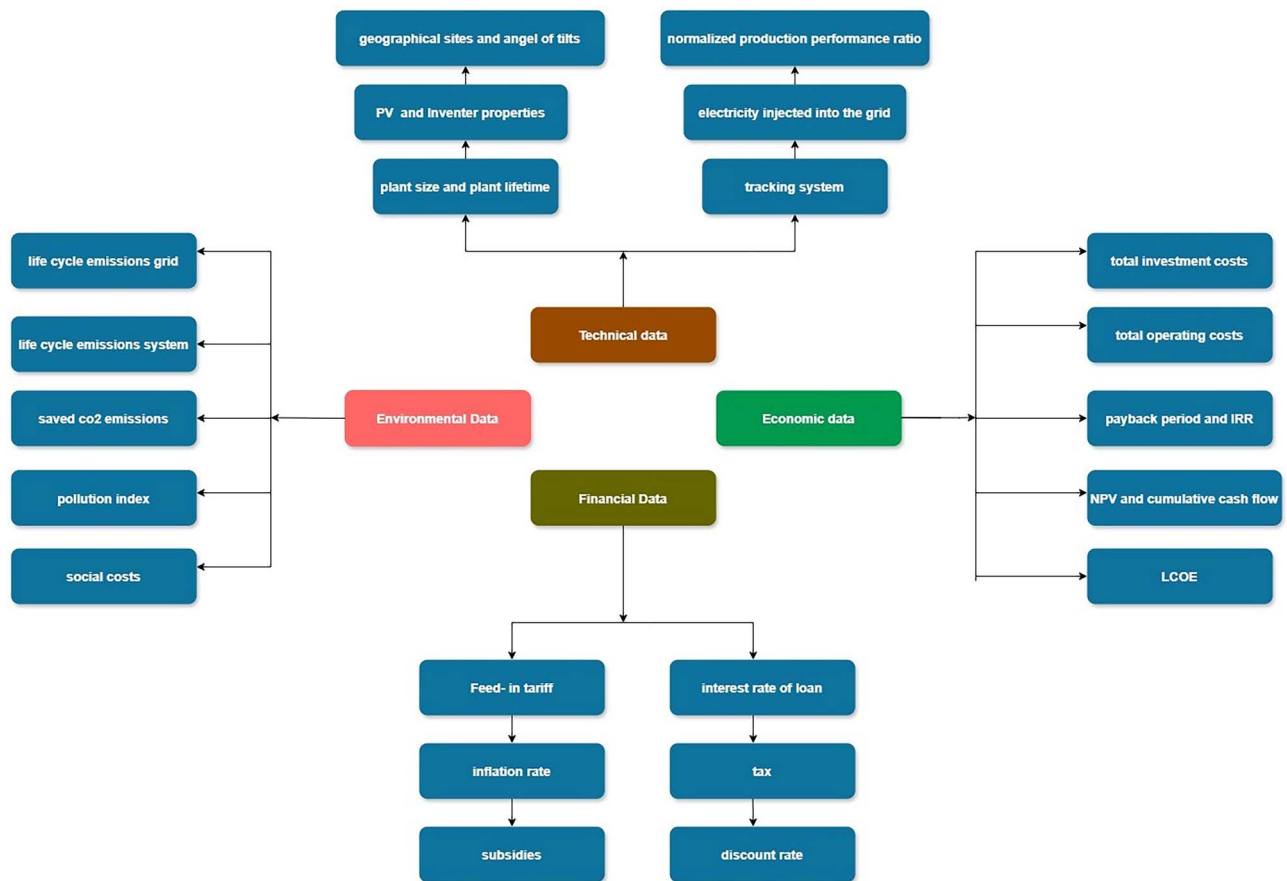


Figure 2. A simplified data flowchart for the solar PV station simulation.

Methodology

Methodology for modeling and simulation

Fig. 2 shows stages in performance modeling, enabling comprehensive analysis of solar system’s effectiveness.

Details of the grid-connected system

PV plants are easy to install, require minimal maintenance, and have low downtime. They are also eco-friendly with no CO₂ emissions. Fig. 3 displays a comprehensive schematic of the system’s components.

Simulation software

PVsyst is a popular and accurate simulation tool for designing PV systems and evaluating electricity production [35]. PVsyst provides detailed data on meteorological conditions, solar resources, PV components, and financial and environmental factors for optimal PV system configuration based on energy demands, viability, and impact [36].

Description of scenarios

Table 1 provides detailed information, and Fig. 4a–c illustrates the design and functionality of each tracker.

Performance indices

The International Electro-Technical Commission (IEC) has set standards (IEC 61724) globally to assess PV system performance, covering various technologies and system types [37].

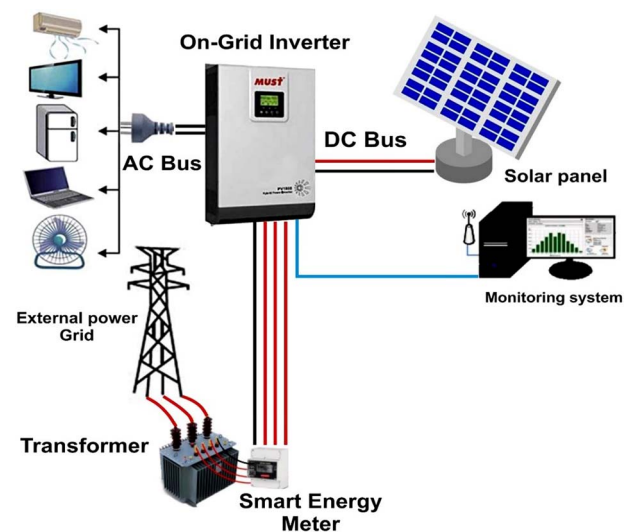


Figure 3. A schematic diagram of PV device (grid-connected) supplying electrical demand.

Table 2 provides the main components of the IEC 61724 performance indices.

PV system losses

Losses occur in distinct components of the PV devices in the form of electricity from solar irradiance absorption through

Table 1. Descriptions of subscenarios depend on tracking features.

System	Descriptions
Scenario 1: No tracker system (fixed tilted)	31° to 32° tilt angle with axis azimuth 0°
Scenario 2: Horizontal single-axis E-W tracker	With axis azimuth 0°, the lowest tilt is -30°, and the highest angle is 80°
Scenario 3: Vertical axis tracker	With an axis azimuth of 30°, the slightest tilt is -120°, and the most significant angle is 120°
Scenario 4: Two-axis E-W tracker	The lowest angle is 10°, the highest tilt is 80°, and the axis azimuth is 30°

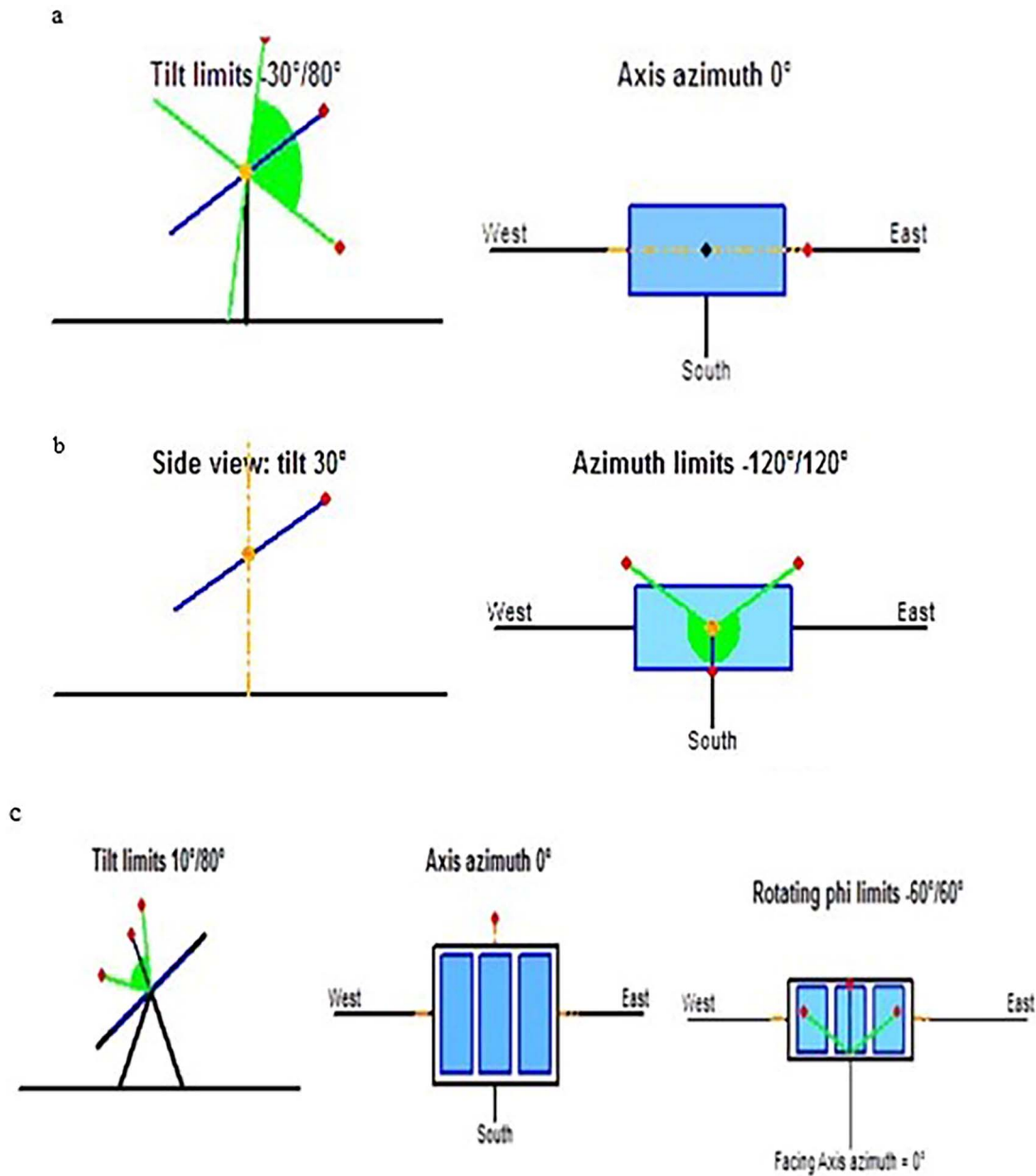


Figure 4. (a) Horizontal single-axis E-W tracker. (b) Vertical axis tracker. (c) Two-axis E-W tracker system.

the receiver panel to electricity delivered to the grid. The following are the most significant losses: L_c (array losses) and L_s (system losses).

- L_c (losses in array)

$$L_c = Y_r - Y_a \tag{9}$$

These losses are classified into two types.

- (a) L_{ct} (heat capture loss).

Heat losses (Equation (10)) are defined as losses when the panel temperature exceeds 25°C. These losses are calculated using the difference between the Y_r and Y_{cr} [47].

$$L_{ct} = Y_r - Y_{cr} \tag{10}$$

- (b) L_{cm} (miscellaneous capture loss).

Table 2. Performance parameters.

Parameter	Description	Equation	Unit	Reference
Y_f	The ultimate yield has been defined as the amount of device adequate AC power over a fixed timeframe divided by the nominal power of the installed plant.	$Y_f = E_{ac}/P_o$ (1)	kWh/kW/day	[38]
Y_r	The reference yield indicates the potential energy generation capacity of a site and the effectiveness of a PV system under specific conditions.	$Y_r = H_r/G_o$ (2)	kWh/kW/day	[39]
Y_a	Array yield is just the ratio of the PV array's electricity provided over a specified timeframe to its nominal power under Standard Test Conditions (STC).	$Y_a = E_{dc}/P_o$ (3)	kWh/kW/day	[40]
PR	The performance ratio is typically calculated as a percentage and can be used to compare of the installed PV panels at different places.	$PR = Y_f/Y_r$ (4)	%	
Specific production	It is often used to evaluate the plant's income potential and compare of the operational performance of various technologies and systems.	Specific production = $\frac{\text{yearly electricity generated}}{P_o}$ (5)	kWh/kWp	[41]
η_{pv}	The PV array efficiency is the amount of electricity converted by the PV panel compared to the available irradiance.	$\eta_{pv} = E_{dc}/H_r * A_m$ (6)	%	[42]
Nominal operating cell temperature (NOCT)	The NOCT of the PV array seems to be the surface temperature achieved by the PV array is subjected to 0.8 kW/m ² of solar irradiance, a temperature of 20°C in the atmosphere, and a wind velocity of 1 m/s.		°C	[43]
η_{inv}	The ratio of P_{ac} (AC power) transfused into the power network by the inverter to P_{dc} (DC power) created by the PV panel.	$\eta_{inv} = P_{ac}/P_{dc}$ (7)	%	[44]
η_{sys}	The instantaneous PV system efficiency is calculated by multiplying PV panel efficiency by inverter efficiency.	$\eta_{sys} = \eta_{pv} * \eta_{inv}$ (8)	%	[45]
E_{ac}	The practical electricity is produced by a PV system over a specific timeframe.		kWh	
FiT	Feed tariffs are fixed prices paid to renewable energy suppliers.		USD/kWh	[46]

String diodes, cables, short circuits, shadow effect, unmatching, low solar irradiation, dust, and losses throughout generating electricity by modules are examples of miscellaneous capture losses (Equation (11)).

$$L_{cm} = Y_{cr} - Y_a \tag{11}$$

- L_s (system losses).

Equation (12) defines system losses as the difference among both Y_a and Y_f . The inverter and passive circuit elements are primarily responsible for these [48]. It is given by the following equation.

$$L_s = Y_a - Y_f \tag{12}$$

Economic evaluation

Net present value

Net present value (NPV) is a financial metric used to assess project profitability, especially for PV investments. It calculates the current value of expected future cash flows using a discount rate to account for the time value of money. A positive NPV indicates a viable project, while a negative NPV suggests potential losses. Equations help calculate NPV by considering net cash flows, project lifespan, and the discount rate. NPV is crucial for objectively evaluating renewable energy investments.

$$NPV = \sum_{n=0}^N \frac{CF_n}{(1+d)^n} \tag{13}$$

Internal rate of return

The internal rate of return (IRR) is the interest rate that makes the NPV of the project zero. If IRR is higher than the discount rate, it is financially viable, otherwise, it is not.

$$NPV = \sum_{n=0}^N \frac{CF_n}{(1+IRR)^n} = 0 \tag{14}$$

Energy cost levelization

LCOE is a vital metric used for comparing economic viability of different power generation technologies, especially cleaner and renewable sources, determining their economic benefits [49]. LCOE (Equation (15)) measures costs of renewable and fossil fuel-based electricity, accounting for project costs, lifespan, and effectiveness.

$$LCOE \left(\frac{\$}{kWh} \right) = \frac{\text{Total lifetime cost} \left(\frac{\$}{Wp} \right)}{\text{Total life cycle electricity yield} \left(\frac{kWh}{Wp} \right)} \tag{15}$$

Environmental assessment

Greenhouse gases (GHGs) are atmospheric gases that absorb and emit infrared radiation, significantly contributing to the greenhouse effect. Effective mitigation of GHG emissions is crucial for maintaining a safe and healthy environment. These emissions are a major driver of climate change, a global

Table 3. Coordinate the locations of the chosen cities in different climatic zones.

Location	Altitude	Latitude	Longitude	Climate zones
Lamerd	415 m	27.36°N	53.16°E	Very hot climate, low mountains
Eqlid	2251 m	30.89°N	52.69°E	Cold climate, high mountains
Shiraz	1529 m	29.60°N	52.54°E	Mild climate

concern that has garnered widespread attention and concern. Iran heavily depends on fossil fuels, especially natural gas, for electricity, resulting in substantial GHG emissions. Solar systems' emissions can be calculated using Equations (16) to (18) to assess their environmental impact and inform sustainable energy policies [48].

$$\text{Produced Emission} = \text{Annual Generation} * \text{Emission CO}_2 \quad (16)$$

$$\text{Replaced Emission} = \text{Annual Generation} * \text{Emission Factor} \quad (17)$$

$$\text{Emission Balance} = \text{Replaced Emission} - \text{Produced Emission} \quad (18)$$

Simulation

Description of case studies

Case studies on three cities in Fars province, Iran (Lamerd, Eqlid, and Shiraz), highlight solar radiation's impact on PV systems (Table 3). It should be noted that the Fars province is located in the southwest of Iran. Analyzing their climate conditions offers insights into system efficiency and adaptability.

Climate information from the city areas studied

The Fars Meteorological Bureau provided the climate information used in this study [50]. Fig. 5a and b displays monthly averages of ambient temperature and wind speed. In addition, Fig. 6a–c shows solar radiation.

Eqlid had the lowest average temperature of 3.2°C in December, while Lamerd had the highest at 36.2°C in July. Monthly average ambient temperatures for Shiraz and Lamerd were also provided. These variations reflect the province's diverse climate, impacting PV cell performance. In Fars province, Lamerd experiences the highest monthly solar irradiance at 293.76 hours, while Eqlid has the lowest at 279.8 hours. Eqlid also has the highest average wind speed at 17 m/s, affecting PV system efficiency and wind energy utilization.

Angle of tilt

Optimizing the tilt angle of PV panels is crucial for maximizing solar radiation absorption, aligning with latitude for optimal exposure [51]. Different tilt angles are important for modeling PV system performance in cities with diverse climates, as shown in Table 4. Further, Table 5 gives the solar panel specifications.

PV panels

For the 5 kW PV project, the proposed solar panels are the Yingli Solar (YL250P-29b) model, each with a rating of 250 W [52]. Yingli Solar panels were selected for their suitability, power, and efficiency. They will be connected in series for the inverter.

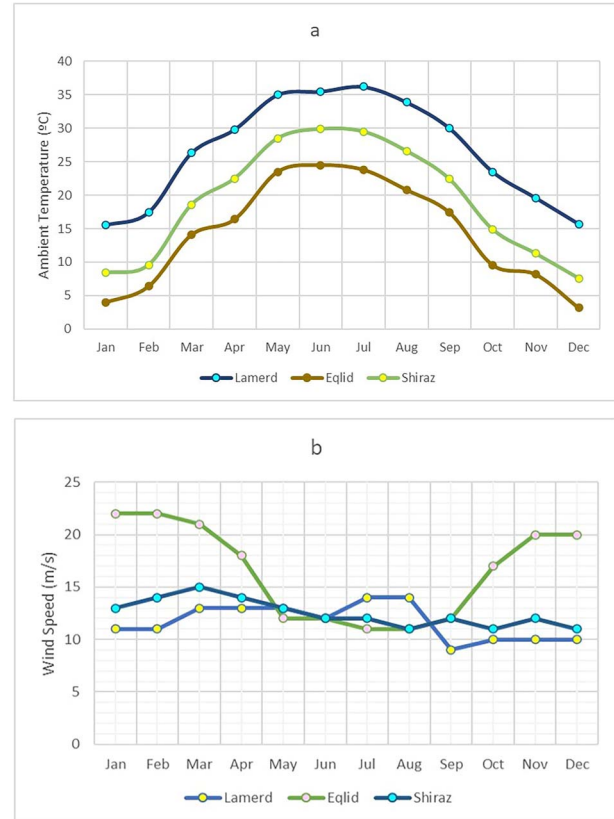


Figure 5. (a) Average monthly ambient temperature. (b) Average monthly wind speed monthly.

Table 4. Solar panel orientation.

N	City Name	Tilt angle
1	Lamerd	31°
2	Eqlid	31°
3	Shiraz	30°

Inverter

The Sunny Boy 4500TL-JP-22 from SMA is chosen as the inverter for the PV system due to compatibility and high efficiency. It operates within a voltage range of 70 to 450 V, aligning with the panels' output. The inverter has an AC output voltage of 202 V and a high efficiency of 96.7%. Detailed specifications can be found in Table 6 for understanding its role in the system's overall efficiency and performance.

Plant layout

A 5 kW solar PV plant needs 32.5 m² of space and can be installed on open land or rooftops, considering sunlight and structural factors. It consists of ten 250 W panels connected in series for consistent current and voltage summation. To achieve 4.5 kW output, two sets of panels are connected in

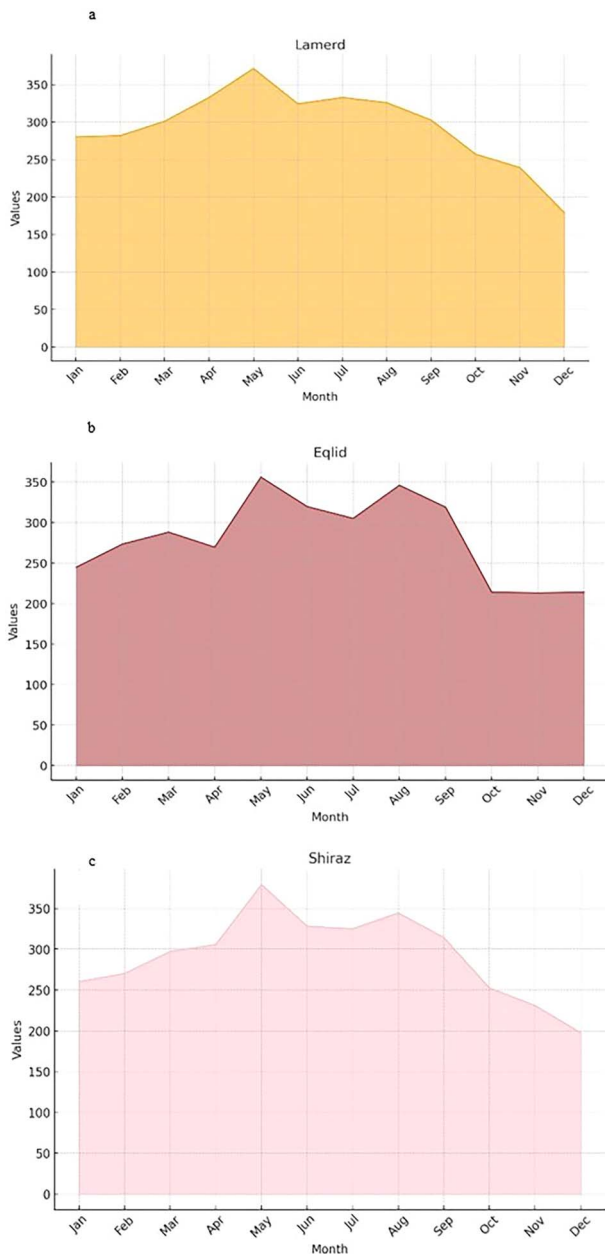


Figure 6. (a) Hourly data on monthly average solar radiation for Lamerd city. (b) Hourly data on monthly average solar radiation for Eqlid city. (c) Hourly data on monthly average solar radiation for Shiraz city

parallel while maintaining voltage for the inverter, using a total of 20 solar modules for energy conversion and power transmission.

Iran’s solar electricity strategies

In 2009, Iran introduced its first feed-in tariff (FiT) scheme, which has since been praised globally for driving the development of renewable energy. The government set the FiT at 0.15 USD/kWh in 2013, demonstrating their dedication to promoting green technology [54]. Iran’s Ministry of Energy has implemented PPAs to incentivize green technologies with favorable tariffs. Table 7 illustrates the guaranteed purchase tariffs for different clean energy sources, highlighting Iran’s pricing policy and economic incentives for renewable energy production.

Table 5. Solar panel specifications [58].

STC	
Panel type	YL250P-29b
P_{max}	250 W
V_{mp}	29.87 V
I_{mp}	8.39 A
V_{oc}	37.67 V
I_{sc}	8.92 A
Panel efficiency	15.3%
NOCT	
P_{max}	182.4 A
V_{mp}	27.2 V
I_{mp}	6.71 A
V_{oc}	34.7 V
I_{sc}	7.21 A
Thermal characteristics	
NOCT	44°C–48°C
Temperature coefficient at P_{max}	-0.42%/°C
Temperature coefficient at V_{oc}	-0.32%/°C
Temperature coefficient at I_{sc}	0.05%/°C
Temperature coefficient at V_{mpp}	-0.42%/°C
Operating conditions	
V_{Max} (system)	600V _{DC} or 1000V _{DC}
Temperature range of operation	-40°C to 85°C

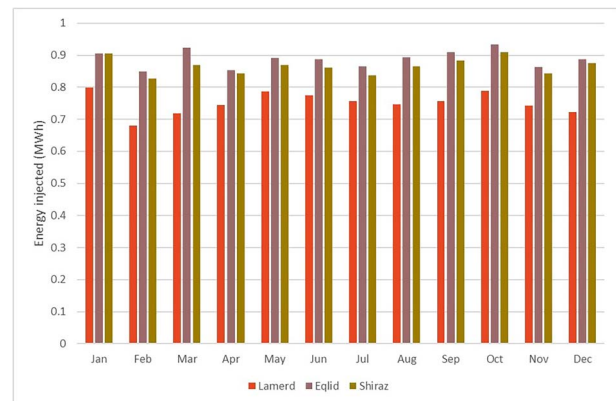


Figure 7. Monthly average electricity injection into the power network [Scenario 1: No tracking system (fixed tilted)].

Discussion and results

This section evaluates the technical, economic, and environmental aspects of a 5 kW rooftop PV plant in seven cities in Fars province, Iran. The analysis considers the plant’s performance, feasibility, viability, and environmental impact, providing a comprehensive understanding of implementing PV systems in urban areas.

Technical evaluation

Scenario 1: No tracking system (fixed tilted)

In Scenario 1, Fig. 7 shows the monthly average electricity generation of a 5 kW PV plant in selected areas of Fars province. In most cities, February had the lowest energy production: 680 kWh in Lamerd, 850 kWh in Eqlid, and 827 kWh in Shiraz. The highest production varied by city: Shiraz and Eqlid peaked in October at 910 and 934 kWh, while Lamerd peaked in January at 800 kWh. This highlights how weather and seasons affect fixed-tilt PV systems.

Table 6. Specifications of inverters [53].

Module type	Sunny Boy 4500TL-JP-22	
Output	Rated output voltage and frequency (Hz)	AC 202 V, 50 Hz/60 Hz
	Max. output current	22.3 A
Input (DC)	Max. generator power	11 250 Wp
	Range of input voltage (V)	70 to 450 V
	Minimum start-up voltage (V)	110 V
	Rated input voltage	330 V
	Range of MPP voltage (V)	160 to 360 V
	Number of input circuits	Two circuits
	Number of terminals /shapes	Two input terminals for each
	Max. input current	Two circuits × 15 A
Efficiency	Max. short-circuit current input A / B	19 A
		96% (max. 96.7%)
Operating ambient conditions		Indoor and outdoor temperature: −25°C to +60°C
		Humidity: 0% to 100% below 2000 m asl
Weight		25.5 kg

Table 7. Guaranteed base purchase prices for generated electricity in Iran using various renewable energy sources [55].

Item	Specification	Cents/kWh
Solar	≤20 kW	5.82
	≤200 kW	5.09
	>200 kW	3.57
Waste heat recovery	-	2.11
Wind farms	>1 MW	3.06
	≤1 MW	4.15
Geothermal	-	3.57
Small hydropower	Thunderstorms on rivers (≤10 MW)	2.77
	Water transfer lines (≤10 MW)	2.37
Biomass	Landfill	2.29
	Biochemical processes (anaerobic digestion)	2.94
	Thermochemical processes (waste incineration, gasification, and pyrolysis)	3.11
Fuel cells	-	3.602
Turbo expander	-	1.165

In terms of electricity contribution to the power network, Lamerd has the lowest annual output, delivering 9.02 MWh, whereas Eqlid leads with the highest contribution, injecting 10.66 MWh into the grid. There is a significant difference in electricity generation capacity across cities due to local geographic and climatic conditions. Comparisons of PV system performance show Eghlid with the highest performance ratio at 80.46% and Lamerd with the lowest at 77.85% (Fig. 8a–c).

Eqlid has the highest rooftop solar PV system performance, with an average production of 5.84 kWh/kWp/day. Lamerd, in a hot climate, has the lowest production at 4.94 kWh/kWp/day (Fig. 9a–c). Temperature differences likely affect efficiency. Comparison of simulation results can be found in Table 8.

Economic evaluation

Scenario 1: No tracking system (fixed tilted)

Investment cost of grid-connected rooftop PV device (Scenario 1).

According to Table 9, the overall cost of purchasing and installing a grid-connected rooftop PV power station in Fars province (Iran) is \$4632.5.

The total operating cost of grid-connected rooftop PV device (Scenario 1)

The overall cost of operation is \$108.32 (Table 10).

In this study, each kilowatt-hour of thermal electricity generated from power stations like combined cycle and gas is assumed to require approximately 0.28 m³ of natural gas. The project in Iran involves a loan at 4% interest rate and 8-year repayment. Natural gas price is 0.025 USD/m³, with an exchange rate of 250 000 Rials per USD. There is a subsidy of 2.86 USD per ton of CO₂ reduction. The model assumes no income tax, uses linear depreciation, and includes specific rates for discount, inflation, and scrap value. A 20% annual increase in guaranteed electricity purchase tariff is considered. Table 11 shows the financial summary for Scenario 1 of grid-connected rooftop solar PV power stations in Eghlid, Lamerd, and Shiraz.

The environmental pollution reduction cost of a grid-connected rooftop solar PV power station.

Over 20 years, Eghlid, Lamerd, and Shiraz rooftop solar power stations will emit 102.02, 84.78, and 99.14 tons of CO₂, resulting in social costs of \$291.77, \$242.47, and \$283.54, respectively. These costs reflect long-term damages like lower crop yields, healthcare costs, and property damage, emphasizing the need to consider environmental and social effects of PV power plants.

Environmental analysis

Table 13 depicts the life cycle emission (LCE) description of the system's major components for calculating CO₂ emissions

Table 8. Grid-connected rooftop PV power plant simulation results in seven Fars province cities (Scenario 1: No tracking system).

Item	Shiraz	Eqlid	Lamerd
System production energy (MWh/year)	10.39	10.66	9.02
Specific production (kWh/kWp/year)	2078	2133	1803
PR (%)	78.47	80.4	77.83
Normalized production (kWh/kWp/day)	5.69	5.84	4.94
Array losses (kWh/kWp/day)	1.32	1.18	1.2
System losses (kWh/kWp/day)	0.24	0.24	0.2

Table 9. Total investment cost of grid-connected rooftop PV device (Scenario 1).

Description	Quantity	Unit price	Total (USD)
PV modules (YL250P-29b) [56]	5000 Wp	0.42 USD/Wp	2100
Mounting structures (2 panels on each structure) [49]	10 units	52.5 USD	525
Inverters (Sunny Boy 4500TL-JP-22) [57]	1 unit	1475 USD/units	1475
AC and DC cables [49]	5000 Wp	0.0625 USD/Wp	312.5
Installation	5000 Wp	0.044 USD/Wp	220
Total investment cost	5000 Wp	0.926 USD/Wp	4632.5

Table 10. The total operating costs rooftop PV device (Scenario 1).

Description	Total (USD)
Maintenance costs	
1% Capital of PV panel (PV module) [60]	21
1% Capital of inverter (AC/DC converter) [60]	14.75
5% Capital of mounting structures (fixed slop) [60]	26.25
Administrative costs (1% of total investment cost)	46.32
Total operating costs	108.32

Table 11. Financial summary for Scenario 1: No tracking system.

Item	Subsidies (\$)	Loans (\$)	NPV (\$)	Payback period (year)	IRR (%)	LCOE (\$/kWh)
Eqlid	291.77	1527.22	5449.47	7	14.28	0.06
Lamerd	242.48	1287.15	3603.65	8.5	11.76	0.07
Shiraz	283.53	1482.8	4696.7	7.5	13.33	0.07

Table 12. The level of pollution index of various pollutants in Iranian power plants, as well as the associated social costs.

Item	CO ₂	CO	NO _x	SPM	CH ₄	SO ₂
Pollution index (g/kWh) [61]	660.65	0.617	2.383	0.11	0.016	1.661
Social cost (USD/ton) [62]	2.86	54	171.5	1228.6	60	521.5

SPM - Suspended particulate matter.

from a rooftop solar PV system. The PVsyst software is used to calculate the LCEs of system components. For all scenarios, the value of the LCE system (replaced emissions tCO₂) is the same.

Scenario 1: No tracking system (fixed tilted)

Equations (16), (17), and (18) were used to calculate the produced emission, replaced emission, and emission balance of the solar plant, respectively. Table 14 shows the LCE grid (produced emissions tCO₂) and emission balance tCO₂ (saved CO₂ emissions) values for Scenario 1. As a result, the cities with the highest and lowest LCE grid (produced emissions tCO₂) and emission balance tCO₂ (saved CO₂ emissions) values are Eqlid and Lamerd, respectively.

Scenario 2: Horizontal single-axis E-W tracking

A single-axis E-W tracking system was used in Scenario 2. LCEs were calculated for Eghlid (120.1 tCO₂), Lamerd (100.48 tCO₂), and Shiraz (116.46 tCO₂). According to Fig. 10a, the city with the lowest LCE grid increases is Lamerd (6.42%). Furthermore, the rate of increase in the LCE grid in Eghlid and Shiraz is the same (7.55%).

Scenario 3: Vertical axis tracking

In Scenario 3, featuring vertical axis tracking, notable differences in LCE grid values (produced emissions tCO₂) and saved CO₂ emissions are observed among cities in Fars province. Eghlid, with 139.1 tons, and Lamerd, with 113.55 tons, represent the highest and lowest LCE grid

Table 13. LCE of components of the rooftop solar PV system details.

Item	Quantity	Gery energy	LCE	Total
Modules	5 kWp	2168 kWh/kWp	1713 kg CO ₂ /kWp	8564 kg CO ₂
Supports	200 kg	6.67 kWh/kg	3.84 kg CO ₂ /kg	767 kg CO ₂
Inverters	One unit	660.8 kWh/units	309 kg CO ₂ /units	309 kg CO ₂
SUM				9.64 tCO ₂

Table 14. Emission balance for grid-connected rooftop solar PV system.

City	LCE grid (produced emissions tCO ₂)	LCE system (replaced emissions tCO ₂)	Emission balance tCO ₂ (saved CO ₂ emissions)
Lamerd	94.42	9.64	84.78
Shiraz	108.78	9.64	99.14
Eqlid	111.66	9.64	102.02



Figure 8. (a) PR for Eqlid. (b) PR for Lamerd. (c) PR for Shiraz (Scenario 1: No tracking system).

values, respectively. In Scenario 3, Eghlid and Lamerd had the highest and lowest increases in LCE grid values at 24.57% and 20.26%, while Shiraz had a 24.32% increase (Fig. 10b)



Figure 9. (a) Normalized production (Y_f) for Eqlid. (b) Normalized production (Y_f) for Lamerd. (c) Normalized production (Y_f) for Shiraz (Scenario 1).

Vertical axis tracking in Scenario 3 resulted in significant increases in LCE grid values and saved CO₂ emissions, varying based on local conditions.

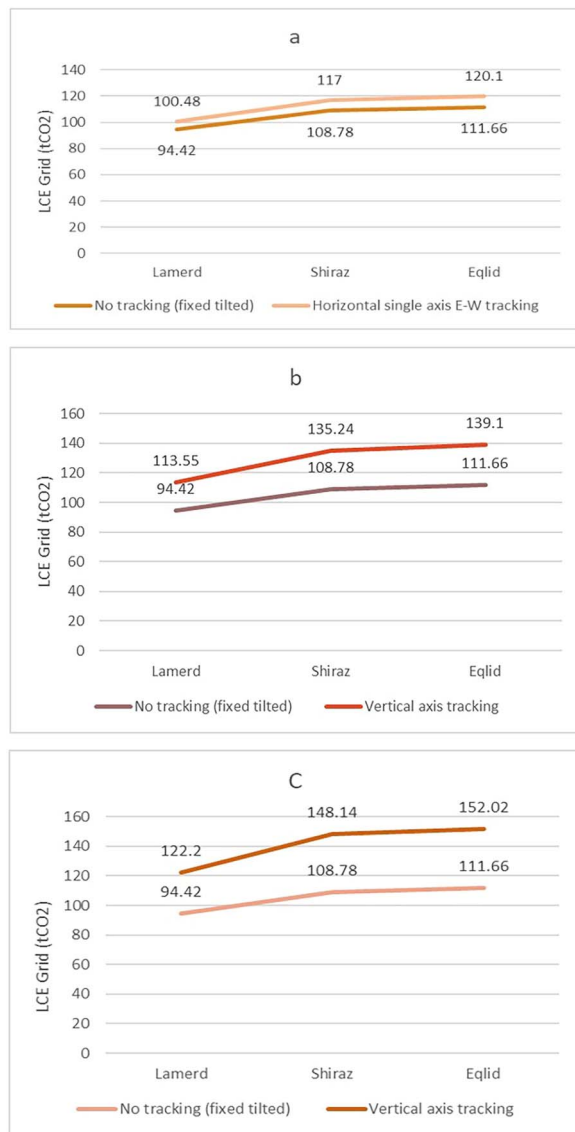


Figure 10. (a) Comparison of LCE grid Scenarios 1 and 2 (produced emissions tCO₂). (b) Evaluation of LCE grid (produced emissions tCO₂) Scenarios 1 and 3. (c) Comparison of LCE grid Scenarios 1 and 4 (produced emissions tCO₂).

Scenario 4: Two-axis E-W tracking system

In Scenario 4, which involves the two-axis E-W tracking system, the LCE grid values (produced emissions in tCO₂) were calculated for several cities using Equations (16) to (18). The estimated LCE grid values are as follows: Eghlid at 152.02 tons, Lamerd at 122.2 tons, and Shiraz at 148.14 tons. As shown in Fig. 10c, Shiraz and Eghlid experienced the largest increases in LCE grid at 36.39%, while Lamerd observed the smallest increase at 29.42%.

Sensitivity analysis

Technical sensitivity analysis

Scenario 2: Single axis horizontal E-W tracker

Using a single-axis horizontal E-W tracker with a tilt range of -30° to 80°, the study found that implementing this tracking system resulted in increased annual average electricity injected into the grid in Fars province. Eghlid had the highest

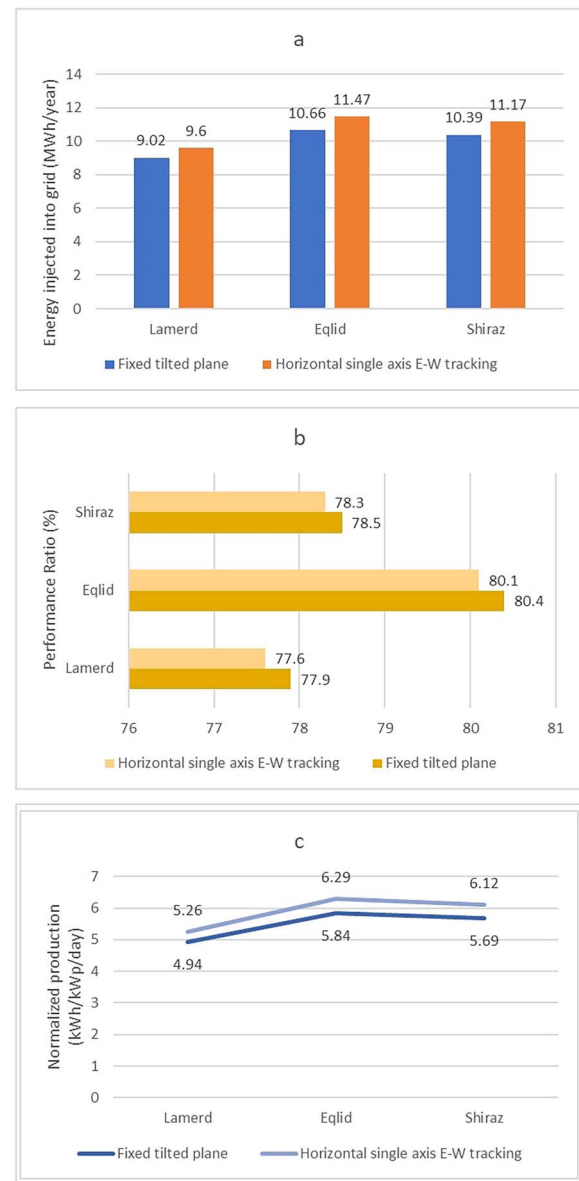


Figure 11. (a) Comparison of electricity injected into the grid in Scenarios 1 and 2. (b) A comparison of the performance ratios of Scenarios 1 and 2. (c) Comparison of normalized production (Y_f) Scenarios 1 and 2.

increase at 7.6%, Lamerd had the smallest increase at 6.43%, and Shiraz showed significant improvements with increase of 7.51%. The study also found a small decline in average performance ratio for all cities, with Lamerd experiencing the largest decrease at -0.38% and Shiraz having the smallest decrease at -0.25%. Implementing horizontal single-axis tracking increased normalized production in all cities, with Eghlid and Lamerd having the highest and lowest Y_f increases at 7.7% and 6.48%. Shiraz saw a rise of 7.56% (Fig. 11a-c). Single-axis horizontal tracking boosted electricity generation and normalized production but slightly reduced performance ratio.

Scenario 3: Vertical axis tracking

The vertical axis tracking system greatly boosts grid electricity injection in Fars province cities. Eghlid sees the highest increase at 24.58%, Lamerd has the lowest increase at

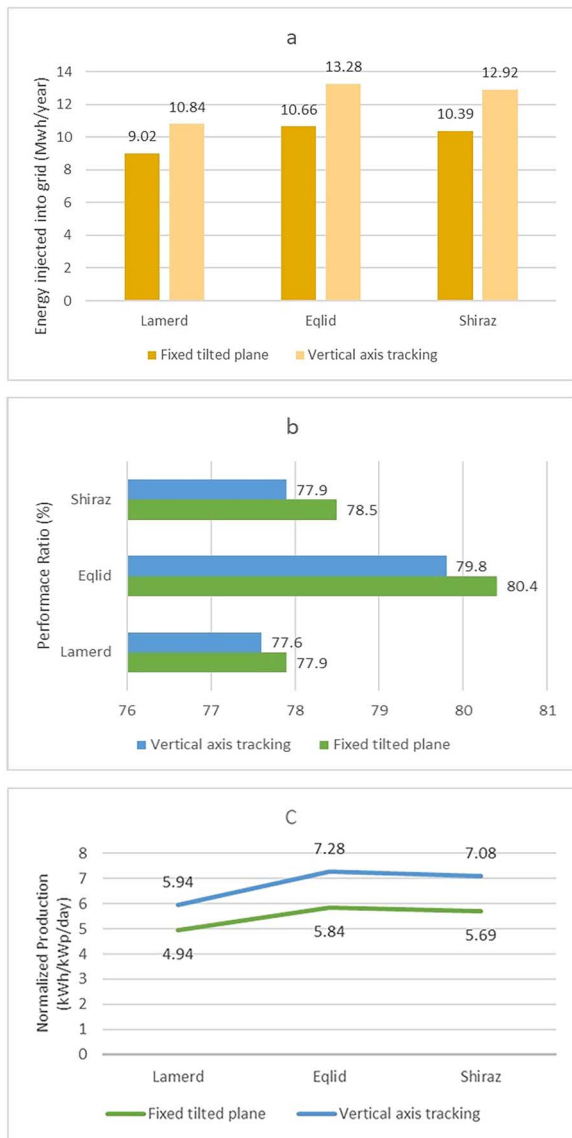


Figure 12. (a) Comparison of electricity injected into the grid in Scenarios 1 and 3. (b) A comparison of the performance ratios of Scenarios 1 and 3. (c) Comparison of normalized production (Y_f) Scenarios 1 and 3.

20.18%, and Shiraz also experiences a substantial increase at 24.35%. However, this system slightly decreases the annual average performance ratio. Shiraz has the largest decrease at -0.76% , while Lamerd has the smallest at -0.38% . Eghlid decreases by -0.74% . Nonetheless, the use of vertical axis tracking leads to a significant increase in normalized production across all selected cities. Eghlid and Lamerd see the highest and lowest increases in production at 24.66% and 20.24%, respectively, while Shiraz’s production rises by 24.43% (Fig. 12a–c). Vertical axis tracking improves electricity generation in urban areas but compromises performance ratio and optimization slightly.

Scenario 4: E-W tracking system with two axes

Implementing a two-axis E-W tracking system (10° – 80° tilt, 0° azimuth limit) greatly boosts grid electricity injection in Fars province. Eghlid sees a 36.21% increase, while Lamerd’s increase is 29.38%. Annual average performance ratio is minimally affected. Eghlid has the most significant

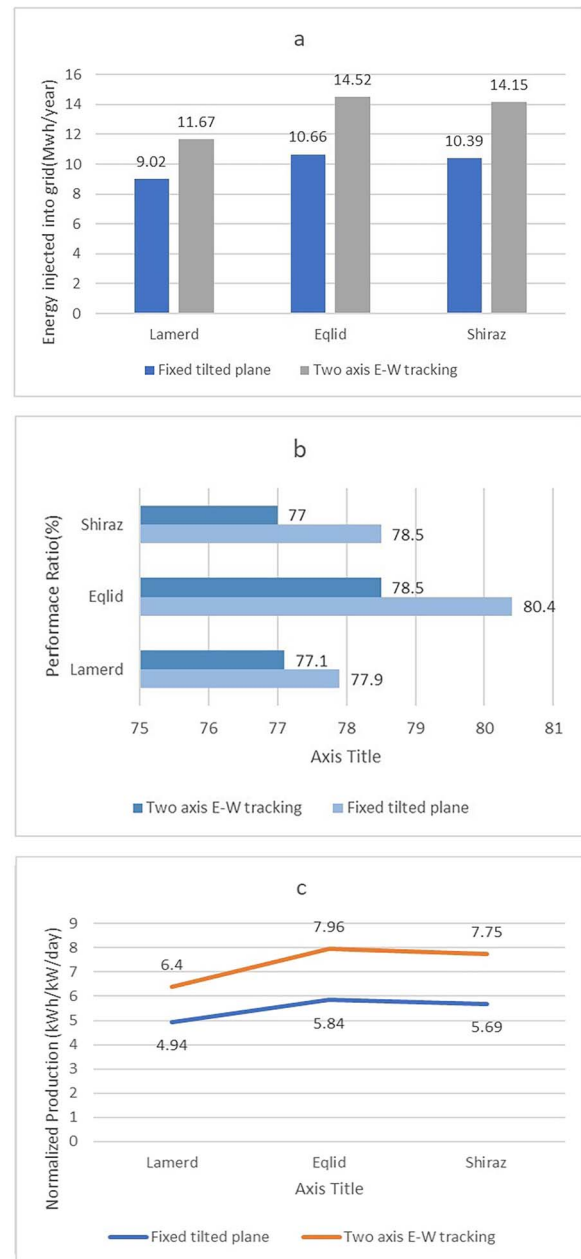


Figure 13. (a) Comparison of electricity injected into the grid in Scenarios 1 and 4. (b) A comparison of the performance ratios of Scenarios 1 and 4. (c) Comparison of normalized production (Y_f) Scenarios 1 and 4.

decrease (-0.024%), Lamerd has the smallest decrease (-0.01%), and Shiraz consistently drops by -0.02% . The two-axis E-W tracking system significantly improves normalized production, with Eghlid and Lamerd achieving 36.3% and 29.55% increases, respectively. Shiraz observes a 36.2% increase (Fig. 13a–c). While electricity generation and normalized production improve, the performance ratio slightly decreases.

Economic sensitivity analysis

Scenario 2: Horizontal single-axis E-W tracking

Investment cost of rooftop PV (grid-connected) device.

Table 15 estimates the overall investment cost of a PV (grid-connected) device at \$5710 for Scenario 2.

Table 15. Overall investment cost of construction for a rooftop PV (grid-connected) device (Scenarios 2–4).

Description	Scenario 2	Scenario 3	Scenario 4
PV modules (YL250P-29b) [56]	2100	2100	2100
Mounting structures (2 panels on each structure) [49]	1550	2100	3250
Inverters (Sunny Boy 4500TL-JP-22) [57, 59]	1470	1470	1470
AC and DC cables [49]	312.5	312.5	312.5
Installation	272.5	282.5	357.5
Total investment cost (USD)	5710	6270	4790

Table 16. The total operating cost of grid-connected rooftop PV devices (Scenarios 2–4).

Description	Scenario 2	Scenario 3	Scenario 4
Maintenance costs			
1% Capital of PV panel [60]	21	21	21
1% Capital of inverter [60]	14.75	14.75	14.75
5% Capital of mounting structures [60]	77.5	105	162.5
Administrative costs (1% of total investment cost)	57.1	62.7	75
Total operating costs (USD)	170.35	203.45	273.25

The total operating cost of the rooftop PV system (grid-connected).

The overall operational cost of grid-connected PV power plants in Scenario 2 is \$170.35, according to Table 16.

The reduction cost of environmental pollutants of grid-connected rooftop PV device.

Over a 20-year lifespan, carbon dioxide emissions from rooftop PV systems in Eghlid, Lamerd, and Shiraz are 110.46, 90.84, and 107.36 tons, respectively, with associated social costs of \$315.91, \$259.80, and \$307.05 reflecting economic impact.

Scenario 3: Vertical axis tracking

Investment cost of rooftop PV (grid-connected) device.

According to Table 15, for Scenario 3, the overall investment cost of a grid-connected PV (grid-connected) device is estimated at \$6270.

The total operating cost of rooftop PV (grid-connected) device.

The overall operating cost of PV solar power plants connected to the grid is estimated at \$203.45 in Table 16, Scenario 3.

The reduction cost of environmental pollutants of grid-connected rooftop PV device.

Over 20 years, rooftop PV systems in Eghlid, Lamerd, and Shiraz will prevent CO₂ emissions: 129.46 tons in Eghlid, 103.91 tons in Lamerd, and 125.6 tons in Shiraz. Social costs associated with emissions will reduce by \$370.25 in Eghlid, \$297.18 in Lamerd, and \$359.22 in Shiraz. Grid-connected PV systems offer environmental and social benefits by mitigating economic and health impacts of carbon emissions.

Scenario 4: Two-axis E-W tracking system

Investment cost of rooftop solar PV device (grid-connected).

The overall investment expense of a grid-connected PV device for Scenario 4 is \$7495, according to Table 15.

The overall operating cost of rooftop PV (grid-connected).

The general operating cost of PV power plants (grid-connected) is estimated at \$273.25 in Scenario 4 (Table 16).

The reduction cost of environmental pollutants of grid-connected rooftop PV.

Over 20 years, grid-connected rooftop PV systems in Eghlid, Lamerd, and Shiraz reduce CO₂ emissions by 142.38, 112.56, and 138.5 tons, respectively, resulting in lowered social costs (\$407.21 for Eghlid, \$321.92 for Lamerd, and \$396.11 for Shiraz). These reductions demonstrate the economic and environmental benefits of using PV systems to address carbon emissions.

Conclusions

Grid-connected PV systems in Iran can alleviate peak load demand by providing alternative energy sources, but they face obstacles like high costs, limited technical development, inadequate training, and lack of support policies. This study examines solar trackers, considering geographic and climatic conditions in Lamerd, Eqlid, and Shiraz to meet residential power demand. Four scenarios, incorporating domestic PPAs, are evaluated. The following are the most essential technical, financial, and environmental outcomes of this work:

- In Scenario 1, Eqlid injected the highest amount (10.66 MWh) and Lamerd the lowest (9.02 MWh) electricity. Eqlid also had the highest normalized production (5.84 kWh/kWp/day), while Lamerd had the lowest (4.94 kWh/kWp/day). Using tracking systems increased electricity injection by 7.56%, 24.67%, and 36.35% in Scenarios 2, 3, and 4, respectively.
- In Eqlid city, it costs \$4632.5 to purchase and install PV equipment. The NPV is \$5449.47 and the IRR is 14.28%. The LCOE is 0.063 USD/kWh (Scenario 1: No tracking system).
- According to LCE, the annual production of 10.66 MWh by the 5 kW power plant installed in Eqlid city will prevent 102.02 tons of carbon dioxide emissions into the atmosphere (Scenario 1: No tracking system).

The study concludes that despite various benefits and incentives including tax-free status, long-term PPAs for the project's lifespan, subsidies for reducing carbon emissions, and loans

with favorable conditions (8-year repayment period and 4% interest rate), none of the four scenarios assessed are economically viable for investment. Solar energy expansion in Iran faces challenges due to insufficient incentives and support. To make it more feasible, the government needs to provide stronger financial incentives, reduce equipment costs, and adopt aggressive renewable energy policies for overcoming economic barriers.

Author contributions

Tao Hai (Investigation [equal], Software [equal], Writing—original draft [equal]), Hussein Jaffar (Conceptualization [equal], Data curation [equal], Software [equal]), Hameed Taher (Methodology [equal], Software [equal], Writing—review & editing [equal]), Ameer Al-Rubaye (Resources [equal], Writing—original draft [equal]), Esraa Said (Conceptualization [equal], Visualization [equal], Writing—review & editing [equal]), Abbas Abdul Hussein (Software [equal], Validation [equal], Writing—review & editing [equal]), Wesam Hassan Alhaidry (Data curation [equal], Formal analysis [equal], Writing—review & editing [equal]), Ameer Idan (Methodology [equal], Resources [equal], Writing—original draft [equal]), and Abozar Salehi (Formal analysis [equal], Methodology [equal], Project administration [equal], Writing—original draft [equal]).

Funding

None declared.

References

1. Abdin Z, Mérida W. Hybrid energy systems for off-grid power supply and hydrogen production based on renewable energy: a techno-economic analysis. *Energy Convers Manage* 2019;196:1068–79. <https://doi.org/10.1016/j.enconman.2019.06.068>.
2. Ma Z, Zhao J, Yu L. et al. A review of energy supply for biomachine hybrid robots. *Cyborg Bionic Syst* 2023;4:0053. <https://doi.org/10.34133/cbsystems.0053>.
3. Dahiru AT, Tan CW. Optimal sizing and techno-economic analysis of grid-connected nanogrid for tropical climates of the Savannah. *Sustain Cities Soc* 2020;52:101824. <https://doi.org/10.1016/j.scs.2019.101824>.
4. Ishaq H, Dincer I. Dynamic analysis of a new solar-wind energy-based cascaded system for hydrogen to ammonia. *Int J Hydrogen Energy* 2020;45:18895–911. <https://doi.org/10.1016/j.ijhydene.2020.04.149>.
5. Xu H, Yang C, Li X. et al. How do fintech, digitalization, green technologies influence sustainable environment in CIVETS nations? An evidence from CUP FM and CUP BC approaches. *Resour Policy* 2024;92:104994. <https://doi.org/10.1016/j.resourpol.2024.104994>.
6. Green MA. Photovoltaic technology and visions for the future. *Prog Energy* 2019;1:013001. <https://doi.org/10.1088/2516-1083/ab0fa8>.
7. Azaizia Z, Kooli S, Elkhadraoui A. et al. Investigation of a new solar greenhouse drying system for peppers. *Int J Hydrogen Energy* 2017;42:8818–26. <https://doi.org/10.1016/j.ijhydene.2016.11.180>.
8. Duan Y, Zhao Y, Hu J. An initialization-free distributed algorithm for dynamic economic dispatch problems in microgrid: modeling, optimization and analysis. *Sustain Energy Grids Netw* 2023;34:101004. <https://doi.org/10.1016/j.segan.2023.101004>.
9. Zheng S, Hai Q, Zhou X. et al. A novel multi-generation system for sustainable power, heating, cooling, freshwater, and methane production: thermodynamic, economic, and environmental analysis. *Energy* 2024;290:130084. <https://doi.org/10.1016/j.energy.2023.130084>.
10. Mokhtar G, Boussad B, Noureddine S. A linear Fresnel reflector as a solar system for heating water: theoretical and experimental study. *Case Stud Therm Eng* 2016;8:176–86. <https://doi.org/10.1016/j.csite.2016.06.006>.
11. Han HJ, Mehmood MU, Ahmed R. et al. An advanced lighting system combining solar and an artificial light source for constant illumination and energy saving in buildings. *Energy Buildings* 2019;203:109404. <https://doi.org/10.1016/j.enbuild.2019.109404>.
12. Kalogirou SA. Solar thermal collectors and applications. *Prog Energy Combust Sci* 2004;30:231–95. <https://doi.org/10.1016/j.pcs.2004.02.001>.
13. Ullivius NC, Rokni M. A study on a polygeneration plant based on solar power and solid oxide cells. *Int J Hydrogen Energy* 2019;44:19206–23. <https://doi.org/10.1016/j.ijhydene.2018.04.085>.
14. Zhu C, Wang M, Guo M. et al. An innovative process design and multi-criteria study/optimization of a biomass digestion-supercritical carbon dioxide scenario toward boosting a geothermal-driven cogeneration system for power and heat. *Energy* 2024;292:130408. <https://doi.org/10.1016/j.energy.2024.130408>.
15. Sampaio PGV, González MOA. Photovoltaic solar energy: conceptual framework. *Renew Sustain Energy Rev* 2017;74:590–601. <https://doi.org/10.1016/j.rser.2017.02.081>.
16. Jahangiri M, Shamsabadi AA, Mostafaeipour A. et al. Using fuzzy MCDM technique to find the best location in Qatar for exploiting wind and solar energy to generate hydrogen and electricity. *Int J Hydrogen Energy* 2020;45:13862–75. <https://doi.org/10.1016/j.ijhydene.2020.03.101>.
17. Temiz M, Javani N. Design and analysis of a combined floating photovoltaic system for electricity and hydrogen production. *Int J Hydrogen Energy* 2020;45:3457–69. <https://doi.org/10.1016/j.ijhydene.2018.12.226>.
18. AlZahrani AA, Dincer I. Design and analysis of a solar tower based integrated system using high temperature electrolyzer for hydrogen production. *Int J Hydrogen Energy* 2016;41:8042–56. <https://doi.org/10.1016/j.ijhydene.2015.12.103>.
19. Besarati SM, Padilla RV, Goswami DY. et al. The potential of harnessing solar radiation in Iran: generating solar maps and viability study of PV power plants. *Renew Energy* 2013;53:193–9. <https://doi.org/10.1016/j.renene.2012.11.012>.
20. Organization RE and EE. Renewable energy and energy efficiency organization. Guaranteed electricity purchase rate. <https://www.satba.gov.ir/en/investment1/guaranteedelectricitypurchaserate-Guaranteed-electricity-purchase-rate> (25 May 2024, date last accessed).
21. Esmaeili H, Almassi M, Ghahderijani M. DPSIR framework to evaluate and analyze Iran's energy security. *Discov Appl Sci* 2024;6:25. <https://doi.org/10.1007/s42452-024-05678-8>.
22. Najafi G, Ghobadian B, Mamat R. et al. Solar energy in Iran: current state and outlook. *Renew Sustain Energy Rev* 2015;49:931–42. <https://doi.org/10.1016/j.rser.2015.04.056>.
23. Bakhshi-Jafarabadi R, Sadeh J, Dehghan M. Economic evaluation of commercial grid-connected photovoltaic systems in the Middle East based on experimental data: a case study in Iran. *Sustain Energy Technol Assess* 2020;37:100581. <https://doi.org/10.1016/j.seta.2019.100581>.
24. Heslop S, MacGill I. Comparative analysis of the variability of fixed and tracking photovoltaic systems. *Sol Energy* 2014;107:351–64. <https://doi.org/10.1016/j.solener.2014.05.015>.
25. Nsengiyumva W, Chen SG, Hu L. et al. Recent advancements and challenges in solar tracking systems (STS): a review. *Renew Sustain Energy Rev* 2018;81:250–79. <https://doi.org/10.1016/j.rser.2017.06.085>.
26. Mirzaei M, Mohiabadi MZ. Comparative analysis of energy yield of different tracking modes of PV systems in semiarid climate conditions: the case of Iran. *Renew Energy* 2018;119:400–9. <https://doi.org/10.1016/j.renene.2017.11.091>.
27. Ismail MS, Moghavvemi M, Mahlia TMI. Design of an optimized photovoltaic and microturbine hybrid power system for

- a remote small community: case study of Palestine. *Energ Conver Manage* 2013;75:271–81. <https://doi.org/10.1016/j.enconman.2013.06.019>.
28. Yang C, Kumar Nutakki TU, Alghassab MA. *et al.* Optimized integration of solar energy and liquefied natural gas regasification for sustainable urban development: dynamic modeling, data-driven optimization, and case study. *J Clean Prod* 2024;447:141405. <https://doi.org/10.1016/j.jclepro.2024.141405>.
 29. Koussa M, Cheknane A, Hadji S. *et al.* Measured and modelled improvement in solar energy yield from flat plate photovoltaic systems utilizing different tracking systems and under a range of environmental conditions. *Appl Energy* 2011;88:1756–71. <https://doi.org/10.1016/j.apenergy.2010.12.002>.
 30. Singh R, Kumar S, Gehlot A. *et al.* An imperative role of sun trackers in photovoltaic technology: a review. *Renew Sustain Energy Rev* 2018;82:3263–78. <https://doi.org/10.1016/j.rser.2017.10.018>.
 31. Honrubia-Escribano A, Ramirez FJ, Gómez-Lázaro E. *et al.* Influence of solar technology in the economic performance of PV power plants in Europe. A comprehensive analysis. *Renew Sustain Energy Rev* 2018;82:488–501. <https://doi.org/10.1016/j.rser.2017.09.061>.
 32. Bahrami A, Okoye CO. The performance and ranking pattern of PV systems incorporated with solar trackers in the northern hemisphere. *Renew Sustain Energy Rev* 2018;97:138–51. <https://doi.org/10.1016/j.rser.2018.08.035>.
 33. Mohammadi K, Naderi M, Saghafifar M. Economic feasibility of developing grid-connected photovoltaic plants in the southern coast of Iran. *Energy* 2018;156:17–31. <https://doi.org/10.1016/j.energy.2018.05.065>.
 34. Antonanzas J, Arbeloa-Ibero M, Quinn JC. Comparative life cycle assessment of fixed and single axis tracking systems for photovoltaics. *J Clean Prod* 2019;240:118016. <https://doi.org/10.1016/j.jclepro.2019.118016>.
 35. Sinha S, Chandel SS. Review of software tools for hybrid renewable energy systems. *Renew Sustain Energy Rev* 2014;32:192–205. <https://doi.org/10.1016/j.rser.2014.01.035>.
 36. Sagani A, Vrettakos G, Dedoussis V. Viability assessment of a combined hybrid electricity and heat system for remote household applications. *Sol Energy* 2017;151:33–47. <https://doi.org/10.1016/j.solener.2017.05.011>.
 37. Srivastava R, Tiwari AN, Giri VK. An overview on performance of PV plants commissioned at different places in the world. *Energy Sustain Dev* 2020;54:51–9. <https://doi.org/10.1016/j.esd.2019.10.004>.
 38. Ibrik IH. Techno-economic assessment of on-grid solar PV system in Palestine. Cruz S, editor. *Cogent Eng* 2020;7:1727131. <https://doi.org/10.1080/23311916.2020.1727131>.
 39. Elhadj Sidi CEB, Ndiaye ML, El Bah M. *et al.* Performance analysis of the first large-scale (15 MWp) grid-connected photovoltaic plant in Mauritania. *Energ Conver Manage* 2016;119:411–21. <https://doi.org/10.1016/j.enconman.2016.04.070>.
 40. Zhu C, Wang M, Guo M. *et al.* Optimizing solar-driven multi-generation systems: a cascade heat recovery approach for power, cooling, and freshwater production. *Appl Therm Eng* 2024;240:122214. <https://doi.org/10.1016/j.applthermaleng.2023.122214>.
 41. Udoh SP, Umoren AM, Okpura NI. Techno-economic analysis of building rooftop photovoltaic power system for lecture hall at Imo State University, Owerri. *Sci J Energy Eng* 2017;4:95–103.
 42. Belmahdi B, Bouardi AE. Solar potential assessment using PVsyst software in the northern zone of Morocco. *Procedia Manuf* 2020;46:738–45. <https://doi.org/10.1016/j.promfg.2020.03.104>.
 43. Attari K, Elyakoubi A, Asselman A. Performance analysis and investigation of a grid-connected photovoltaic installation in Morocco. *Energy Rep* 2016;2:261–6. <https://doi.org/10.1016/j.egy.2016.10.004>.
 44. Manoj Kumar N, Sudhakar K, Samykano M. Techno-economic analysis of 1 MWp grid connected solar PV plant in Malaysia. *Int J Ambient Energy* 2019;40:434–43. <https://doi.org/10.1080/01430750.2017.1410226>.
 45. Gao J, Wang Z, Li X. *et al.* Investigation of a novel scheme utilizing solar and geothermal energies, generating power and ammonia: exergoeconomic and exergoenvironmental analyses and cuckoo search optimization. *Energy* 2024;298:131344. <https://doi.org/10.1016/j.energy.2024.131344>.
 46. Tribioli L, Cozzolino R. Techno-economic analysis of a stand-alone microgrid for a commercial building in eight different climate zones. *Energ Conver Manage* 2019;179:58–71. <https://doi.org/10.1016/j.enconman.2018.10.061>.
 47. Cocco DS, Costa AMS. Effect of a global warming model on the energetic performance of a typical solar photovoltaic system. *Case Stud Therm Eng* 2019;14:100450. <https://doi.org/10.1016/j.csite.2019.100450>.
 48. Ahmed N, Naveed Khan A, Ahmed N. *et al.* Techno-economic potential assessment of mega scale grid-connected PV power plant in five climate zones of Pakistan. *Energ Conver Manage* 2021;237:114097. <https://doi.org/10.1016/j.enconman.2021.114097>.
 49. Fars Meteorological Bureau. <https://www.farsmet.ir/Default.aspx> (25 May 2024, date last accessed).
 50. Fars Meteorological Bureau. *Reporting monthly statistics of Fars province*. <https://www.farsmet.ir/ReportAmar.aspx> (12 April 2022, date last accessed).
 51. Hafez AZ, Soliman A, El-Metwally KA. *et al.* Tilt and azimuth angles in solar energy applications—a review. *Renew Sustain Energy Rev* 2017;77:147–68. <https://doi.org/10.1016/j.rser.2017.03.131>.
 52. manualzz. Yingli YL250P-29b Data Sheet. <https://manualzz.com/doc/11503449/yingli-yl250p-29b-data-sheet> (25 May 2024, date last accessed).
 53. Unboundsolar. SMA Sunny Boy Review: Pricing, Specs, Pros and Cons (2021 Edition). <https://unboundsolar.com/blog/sma-sunny-boy-review> (4 January 2021, date last accessed).
 54. Renewable energy and energy efficiency organization (SATBA). *Tariff*. <http://www.satba.gov.ir/fa/guidance/guidance/guidance1/tariff> (24 October 2021, date last accessed).
 55. Walker H. *Best Practices for Operation and Maintenance of Photovoltaic and Energy Storage Systems*; 3rd Edition. 2018, National Renewable Energy Lab. (NREL), Golden, CO (United States). <https://research-hub.nrel.gov/en/publications/best-practices-for-operation-and-maintenance-of-photovoltaic-and-> (24 May 2024, date last accessed).
 56. Iran's energy balance. 2017. <https://irandataportal.syr.edu/wp-content/uploads/1394-1.pdf> (24 May 2024, date last accessed).
 57. Hanafizadeh P, Eshraghi J, Ahmadi P. *et al.* Evaluation and sizing of a CCHP system for a commercial and office buildings. *J Build Eng* 2016;5:67–78. <https://doi.org/10.1016/j.job.2015.11.003>.
 58. secondsol. Yingli - YL 250 P-29b Solarmodule 250W. <https://www.secondsol.com/en/anzeige/19429/pv-module/kristallin/poly/yingli/yl-250-p-29b-solarmodule-250w> (17 April 2022, date last accessed).
 59. Sunmarket. SUNNY BOY 4500TL-JP / 5400TL-JP. http://sunmarket.hu/wp-content/uploads/2020/01/SUNNY_BOY_4500TL-JP-5400TL-JP_angol.pdf (15 January 2021, date last accessed).
 60. Walker H. *Best Practices for Operation and Maintenance of Photovoltaic and Energy Storage Systems*, 3rd Edition. 2018. <https://doi.org/10.2172/1489002>.
 61. Iran's energy balance, 2017
 62. Hanafizadeh P, Eshraghi J, Ahmadi P. *et al.* Evaluation and sizing of a CCHP system for a commercial and office buildings. *Journal of Building Engineering* 2016;5:67–78. <https://doi.org/10.1016/j.job.2015.11.003>.